Thermal-loading-induced tunable flattening dynamics of flexible single-walled carbon nanotubes

2008 J. Phys.: Condens. Matter 20 445223

(http://iopscience.iop.org/0953-8984/20/44/445223)

IOP PUBLISHING JOURNAL OF PHYSICS: CONDENSED MATTER

J. Phys.: Condens. Matter **20** (2008) 445223 (7pp) doi:10.1088/0953-8984/20/44/445223

Thermal-loading-induced tunable flattening dynamics of flexible single-walled carbon nanotubes

Bin-Hao Chen[1], Shing Cheng Chang[2], Ming-Shan Jeng[1] and Cha'o-Kuang Chen[2]

[1] Industrial Technology Research Institute, Energy and Environment Laboratories, C600, Rm. 511, No. 8, Gongyan Road, Liujia Shiang, Tainan County 734, Taiwan, Republic of China

[2] Department of Mechanical Engineering, National Cheng-Kung University, Tainan, 701, Taiwan, Republic of China

E-mail: bhchen@itri.org.tw

Received 13 March 2008, in final form 9 September 2008
Published 10 October 2008
Online at stacks.iop.org/JPhysCM/20/445223

Abstract

Non-equilibrium molecular dynamics simulations are performed to investigate the cross-sectional deformation of single-walled carbon nanotubes (SWCNTs) under axial thermal loadings of 0.51–4.65 K Å^{-1}. It is shown that, given a thermal loading of sufficient intensity, the initial round cross section of the hot end of the nanotube transits through a series of triangular-like states to a flattened, rectangular configuration. As time elapses, the cross section oscillates between two fully perpendicular flattened states at a frequency which increases linearly with the intensity of the applied thermal load. The diameter of the passing pore within the flattened SWCNT is smaller than that of the original cross section, but is independent of the intensity of the thermal load. The simulation results suggest that the structural deformation of the SWCNT induced by the application of a thermal load can be exploited to realize nanoscale mechanical systems/motors such as nanoclamps, for example, or active fluid transport devices for molecular selection or thermal pumping applications.

M This article features online multimedia enhancements

(Some figures in this article are in colour only in the electronic version)

Nomenclature

F	Interaction force
K_{cr}	Force constant of stretch potential
$K_{c\theta}$	Force constant of bend potential
m	Mass of the atom
r_{ij}	Distance between atoms i and j
r_c	Nearest atomic distance at equilibrium
dt	Time steps
T	Temperature
U_{bond}	Potential of C–C bonding
$U_{\mathrm{van\ der\ Waals}}$	Potential of C–C van der Waals interaction
v	Velocity of atoms
$\varepsilon_{\mathrm{cc}}$	Cohesion energy
σ_{cc}	Distance of equilibrium state
ξ_{ij}	Morse bond of C–C interaction
θ_{ijk}	Bending angle

1. Introduction

Carbon nanotubes (CNTs) can be viewed as graphite sheet(s) rolled up into tiny tube form. These elongated nanotubes usually have a diameter ranging from a few ångströms to tens of nanometers. Graphite semiconductor CNTs can be either metallic or semi-conducting, depending upon their diameter and helicity arrangement of graphite rings [1–3]. Due to unique mechanical, electrical, magnetic, optical and thermal properties, carbon nanotubes (CNTs) are candidates

for applications as fillers in composite materials to enhance mechanical behavior [4, 5] and thermal transport [6, 7]. CNTs have been used in many areas, such as an electron emitter in field emission displays, reinforcement filler in nanocomposite materials, scanning probe microscopy tips, actuators and sensors, and as a molecular scale component in micro/nanodevices [8]. The use of CNTs, either in aligned or non-aligned form, such as the reinforcement agent for making advanced polymer composites and biosensors in biomedical devices, inevitably requires modification of their surface characteristics to meet specific requirements for particular applications [9–11]. Recent experiments for thermal conductivity report that the thermal conductivity of organic fluids or polymers when filled with 1% by volume of CNT [6, 7] more than doubled. Nanotube high thermal conductivity is attributed to these increases. Performing thermal conduction measurements is still challenging due to the technological difficulties of synthesizing high-quality and well-ordered nanotubes. Thus, observing theoretical descriptions of thermal conductivity and various thermal loading influences induced on structural deformations is essential.

The SWCNT diameters fall into the nanometer regime, but can be hundreds of micrometers long. Nanotube properties are influenced by its atomic arrangement. The physical and chemical behavior of an SWCNT is therefore related to its unique structural features [12].

This work uses the model adopting Morse bending, a harmonic cosine and van der Waals carbon–carbon interaction to study the transient behavior of carbon nanotubes subjected to different thermal loadings. The carbon nanotube consists of 1440 atoms, corresponding to a nanotube length of ∼100 Å a diameter of 10.8 Å and subjected to different temperature gradients.

Molecular dynamics simulations and nanotransport devices are currently used to investigate atomistic mechanisms, successfully applied in interface and nanomechanics behavior.

One of the most interesting aspects of CNTs is their nanometer-scale hollow-tube-like structure. CNTs are conventionally thought to have a right-cylinder-type configuration. However, experimental and computational studies [4, 13–16] have shown that, given a sufficient diameter, nanotubes have a stable barbell-like flattened structure. The closest wall–wall separation in this flat configuration is roughly equal to the separation of two graphite planes, i.e. 3.4 Å. The flattened structure occurs when the tube diameter increases to such an extent that the attractive van der Waal forces acting between the tube walls exceed the bonding forces acting between neighboring atoms in the nanotube structure. The literature contains many examples of molecular dynamics (MD) simulations designed to clarify the structural phenomena of nanotubes [17–20]. López *et al* studied the coalescence of tubes and the deformation of carbon nanotube ropes under thermal treatment [21]. Gang Wu *et al* investigated heat conduction in intramolecular junctions by using molecular dynamics method; they found that heat conduction is asymmetric [22]. However, previous investigations into the thermal properties of CNTs have not discovered the effects of thermally induced periodic structural flattened deformation. Due to the technological difficulties involved in synthesizing high-quality, well-ordered nanotubes, it is next to impossible to carry out thermal conduction measurements using experimental techniques. Thus, in attempting to clarify the effects of thermal loading on the structural deformation of CNTs, simulation techniques such as the MD scheme are inevitably required.

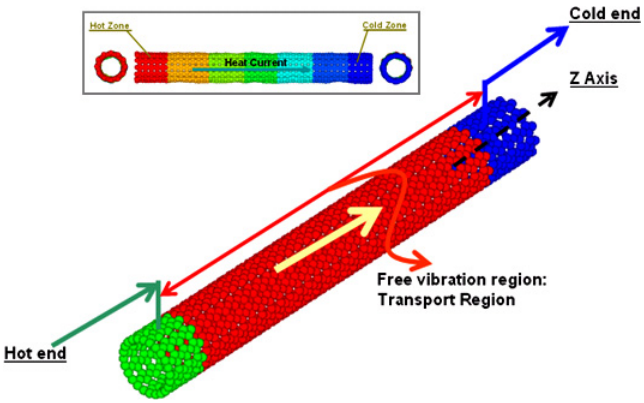

Figure 1. Simulation model. A CNT simulation model with hot and cold ends.

The current study performs non-equilibrium MD simulations to investigate the thermally induced dynamic structural deformation of SWCNTs under axial thermal loads ranging from 0.51 to 4.65 K Å^{-1}. The thermal loading can be applied by pulsed infrared laser heating as in the nano-imprinting technique [23]. The simulations focus on two key aspects, namely (1) the correlation between the SWCNT cross-sectional profile and the intensity of the applied thermal load and (2) the time-dependent dynamics of the deformed SWCNT cross section.

2. Physical model

The present study considers three-dimensional transient-state heat transfer in an armchair structure single-wall carbon nanotube. Figure 1 shows that the system imposes hot and cold walls to simulate non-equilibrium behavior. Average reservoir temperatures are maintained at the desired temperature by applying the Nosé-Hoover thermostat. As shown, the model comprises three distinct regions, namely hot and cold reservoirs at either end of the SWCNT and an intermediate region comprising free vibration atoms which transport heat from the hot end to the cold end. The z direction is the axial direction of the tube. It cannot be both free for real SWCNTs: however, the cold end of SWCNTs with low kinetic energy acts as a fixed end. Therefore, the simulation results are equal to the fixed cold end.

2.1. Potential functions

The carbon nanotube is modeled by terms describing the Morse bond and harmonic cosine of the bonding angle as [24, 25]

$$U\left(r_{ij},\theta_{ijk}\right)=K_{\mathrm{cr}}\left(\xi_{ij}-1\right)^2+\tfrac{1}{2}K_{c\theta}\left(\cos\theta_{ijk}-\cos\theta_{\mathrm{C}}\right)^2 \quad (1)$$

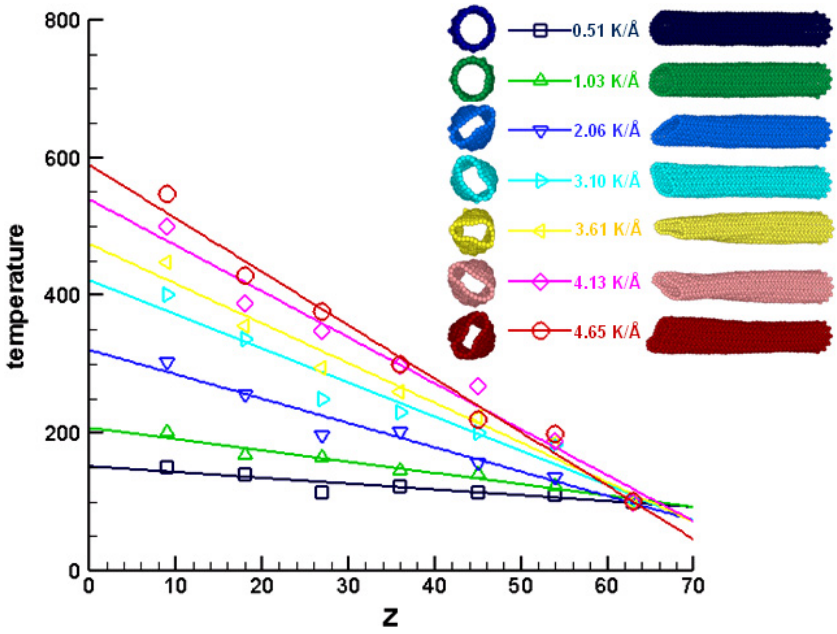

Figure 2. SWCNT hot end configuration. Effects of axial thermal loads of different intensities on temperature gradient induced within SWCNTs and hot end configuration.

where

$$\xi_{ij} = \mathrm{e}^{-\gamma(r_{ij}-r_{\mathrm{c}})}$$

θ_{ijk} represents all possible bending angles and r_{ij} represents all distances between bonded atoms. K_{cr} and $K_{c\theta}$ are the force constants of the stretch and bend potentials, respectively. r_{c} and θ_{C} are the corresponding reference geometry parameters. The Morse stretch and angle bending parameters were first given by Guo *et al* [25]. These parameters, listed in table 1, were originally derived to describe the geometry and phonon structure of graphite and fullerene crystals.

A Lennard-Jones term is added to the nanotube potential to account for the steric and van der Waals carbon–carbon interaction:

$$U\left(r_{ij}\right) = 4\varepsilon_{\mathrm{cc}}\left[\left(\frac{\sigma_{\mathrm{cc}}}{r_{ij}}\right)^{12} - \left(\frac{\sigma_{\mathrm{cc}}}{r_{ij}}\right)^{6}\right]. \qquad (2)$$

Excluding 1–2 and 1–3 pairs, the parameters $\varepsilon_{\mathrm{cc}}$ and σ_{cc} are taken from the so-called universal force field (UFF) [26].

The physical model scale lying at the microscopic level necessitates introducing some dimensionless units into the simulation activity. In all MD simulations, 1 fs time step is employed and 40 ps initial MD is used to equilibrate the systems. After equilibration, 400 ps constant energy (NVE) simulation is conducted. The heat current is calculated every time step. Average temperatures in all simulations exerted by different thermal loadings are calculated by averaging the free vibration atoms' thermal states.

3. Results and discussion

The present dynamic behavioral analysis of cross-sectional deformation of single-walled carbon nanotubes (SWCNTs) considered the periodic flattening phenomena under axial thermal loadings.

Table 1. Parameters for the carbon interaction potential used in the simulation.

$K_{\mathrm{cr}} = 478.9$ kJ mol^{-1} Å^{-2}	$r_{\mathrm{c}} = 1.418$ Å
$K_{c\theta} = 562.2$ kJ mol^{-1}	$\theta_{\mathrm{C}} = 120.00°$
$\varepsilon_{\mathrm{cc}} = 0.4396$ kJ mol^{-1}	$\sigma_{\mathrm{cc}} = 3.851$ Å

Figure 2 illustrates the effects of the applied thermal load on the temperature distribution and structural deformation of the SWCNT. The graph indicates the temperature gradient established along the length of the nanotube under each of the thermal loads. It can be seen that the hot end temperature varies from around 150 K under a thermal load of 0.51 K Å^{-1} to just under 600 K under a thermal load of 4.65 K Å^{-1}. Meanwhile, the schematic illustrations presented to the right of the graph indicate the corresponding cross-sectional profiles of the hot end of the SWNCT and present a side view of each of the deformed tubes. Under lower thermal loads, i.e. 0.51 and 1.03 K Å^{-1}, the hot end of the tube retains a circular cross section. However, as the thermal load is increased to 2.06 K Å^{-1} and beyond, a prominent structural flattening effect is observed. A previous study has shown that a CNT transits to a stable flattened structure when its diameter is sufficiently large that the forces between the opposing walls of the tube are greater than those bonding the individual carbon atoms within the nanotube structure. However, the present results show that CNTs also adopt a flattened structure given a sufficient thermal input. As shown in figure 2, the thermal loadings considered in the current simulations are of insufficient intensity to achieve a significant increase in the kinetic energy of the atoms at the cold end of the nanotube, and hence the cross section retains a stable round configuration. However, given a thermal loading

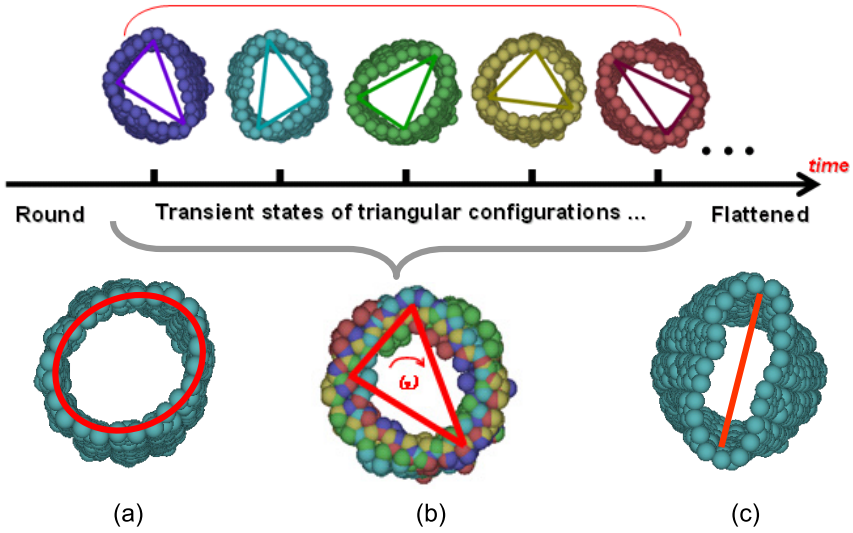

Figure 3. Transition states' evolution. Dynamic evolution of the SWCNT hot end cross section from an initial round configuration to a final flat structure. (Note that the triangular states evolve in a clockwise direction, as shown in animation #1 (available at stacks.iop.org/JPhysCM/20/445223)).

of 2.06 K Å^{-1} or more, the resulting energy contribution to the atoms at the hot end of the SWCNT renders the flattened nanotube structure more energetically favorable, and hence structural deformation takes place.

Figure 3 presents the evolution of the hot end cross section of an SWCNT from its initial round configuration to a final flattened state. As shown in the upper panel of the figure, the cross section evolves through a series of triangular-like states during the deformation process (see also animation #1, supplementary information (available at stacks.iop.org/JPhysCM/20/445223)). From an inspection of the bond angles, it is found that the triangular-like structures rotate in the clockwise direction as the deformation process proceeds. The results suggest that the nanotube cross section transits to a triangular configuration in order to relax the compression effect induced by the applied thermal load.

As shown in figures 2 and 3, the application of an axial thermal load to the SWCNT causes a compression of the nanotube walls. The CNT structure's elasticity will give a repulsive force. As the walls are repelled, the nanotube quickly opens up and the interior volume increases. The kinetic energy of the nanotube walls is converted into potential energy as the nanotube stretches. This results in the nanotube overshooting its initial round configuration and becoming flattened once again. However, the direction of the flattened cross section is perpendicular to that in the previous case. The nanotube subsequently oscillates periodically between these two fully perpendicular flattened states, as shown in the upper panel of figure 4 (see also animation #2, supplementary information (available at stacks.iop.org/JPhysCM/20/445223)). The lower panel in figure 4 illustrates the effect of the thermal loading intensity on the frequency of the structural oscillations of the SWCNT. It can be seen that the period between the two flattened states decreases as the intensity of the thermal loading is increased, i.e. from 8.53 ps at a loading of 2.06 K Å^{-1} to 5.95 ps at a loading of 4.65 K Å^{-1}. Although not presented here, in dynamic simulations performed at a higher thermal loading of ∼5.17 K Å^{-1}, corresponding to a hot end temperature of 650 K, the tube structure collapsed as a result of the high temperature gradient. The simulation results presented in figure 4 indicate that the diameter of the passing pore is smaller than that of the original cross section of the SWCNT, but is essentially insensitive to the magnitude of the thermal loading.

3.1. Melting and clustering mechanism of SWCNTs at high thermal loading

Figure 5 gives us an overall physical picture of the melting process of SWCNTs (see also animation #3, supplementary information (available at stacks.iop.org/JPhysCM/20/445223)). Current results show that the melting of SWCNTs starts from the boundary atoms. The cutoff distance for covalent C–C bonds is given at the value of 2.5 times the C–C bond equilibrium distance. An observation of figures 5(a) and (b) reveals that the point defect moves along the tube's Z-axis direction. Interestingly, when thermal loading is applied, the boundary atoms transform into a pentagonal structure, and then a point defect is present (see figure 6; also animation #4, supplementary information (available at stacks.iop.org/JPhysCM/20/445223)). The presence of a pentagonal defect in the tube may act as a driving force and leads to promote melting. Pentagonal defects can be produced by thermal treatment at the relatively high temperature gradient (>5.17 K Å^{-1}). The defect formation discovered in the current study is similar to the Stone–Wales phenomena. At the relatively high temperature gradient (>5.17 K Å^{-1}), the pentagonal defect can be created associated with a heptagonal ring [27, 28]. Due to the high temperatures, defects have a high mobility and diffuse throughout the tube, then induce the structural phase transition. These snapshots show the atom

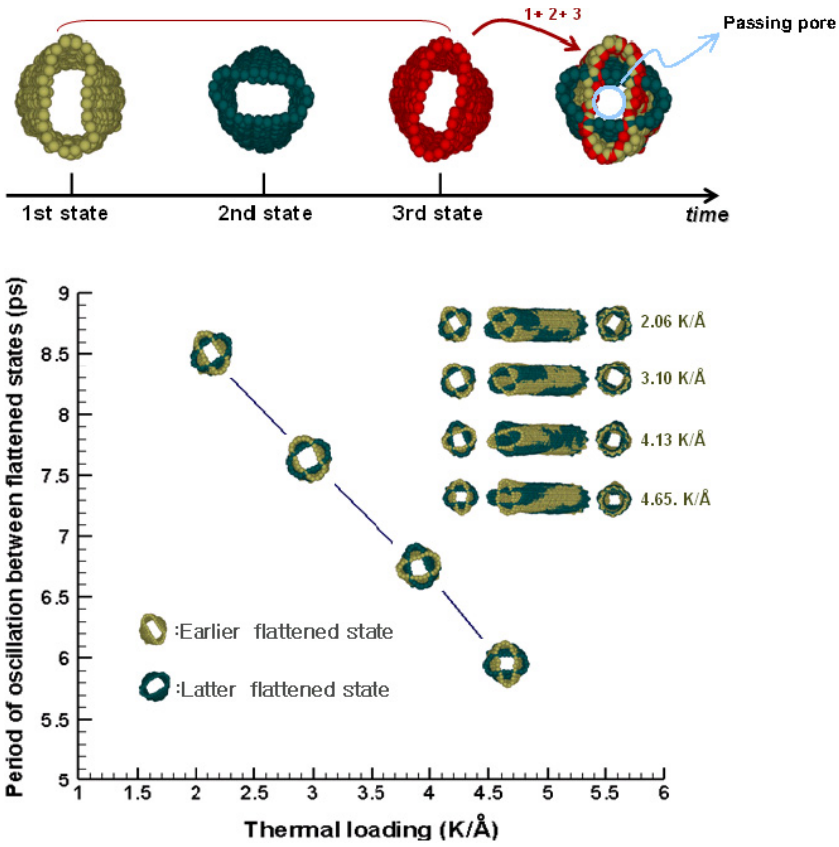

Figure 4. SWCNT flattening dynamics. The nanotube cross section exhibits a dynamic periodic oscillation between two fully perpendicular flattened states. The earlier flattened state is shown in brown; the latter in green. From inspection, the diameter of the passing pore is found to be approximately 2 Å smaller than that of the original SWCNT (∼10.8 Å).

dislocation—defect formation—then the melting process and particle vaporization. In the current study, the heating rate is 2.5–20 K ps^{-1}. The value of the heating rate is still sufficient for the current to reach a thermal equilibrium state without influence of ant transient thermal impact effect.

To further illustrate the melting phenomena of SWCNTs subjected to thermal treatment, figure 7 shows the radical distribution function (RDF) of SWCNTs at different thermal loadings. In order to characterize the structure of CNTs under different thermal loading, the RDF curves are generated by the following definition [29]:

$$g(r) = \frac{V}{N^2}\left\langle \sum_i \sum_{j \neq i} \delta\left(r - r_{ij}\right)\right\rangle.$$

Each curve takes 400 ps timescale average over pairs.

At low thermal loadings, the crystalline structure is highly stable. With increasing thermal loading higher than 5.17 K Å^{-1} the peaks are broadened and lowered. Finally, the crystal order is broken and part of the melting occurs. Some peaks are nearly lost. The shape of the RDF at the thermal loading 5.17 K Å^{-1} implies that coexistence of liquid and crystal is presented. It should be noticed that only parts of the C–C bonds are broken when SWCNTs reach the melting temperature. This paper has performed a series of molecular dynamics simulations to investigate the structural deformation of SWCNTs under the effects of an axial thermal load. The results have shown that, given a sufficient thermal loading intensity, the original round cross section of the hot end of the nanotube evolves through a series of triangular transitional states to a flattened configuration. The flattened cross section exhibits a periodic oscillation between two fully perpendicular flattened states over time. The frequency of the structural oscillation increases approximately linearly as the intensity of the thermal loading is increased. However, the diameter of the passing pore in the deformed nanotube is independent of the thermal loading intensity. Overall, the results presented in this study demonstrate the potential for exploiting the thermally induced cross-sectional deformation of SWCNTs to realize tunable actuators and filters for nanotransportation applications or nanoscale mechanical systems/motors such as nanoclamps. Furthermore, the cross-sectional deformation of the SWCNT results in a change in its field emission properties. Consequently, the results also suggest the feasibility of employing a thermal modulation technique to achieve such SWCNT-based applications as tunable bundle spacing to adjust the turn-on field strength and current density, which can indicate further optimization of spacing in the arrays of CNTs.

4. Conclusions

This study has attempted to clarify the cross-sectional flattening dynamics of single-walled carbon nanotubes

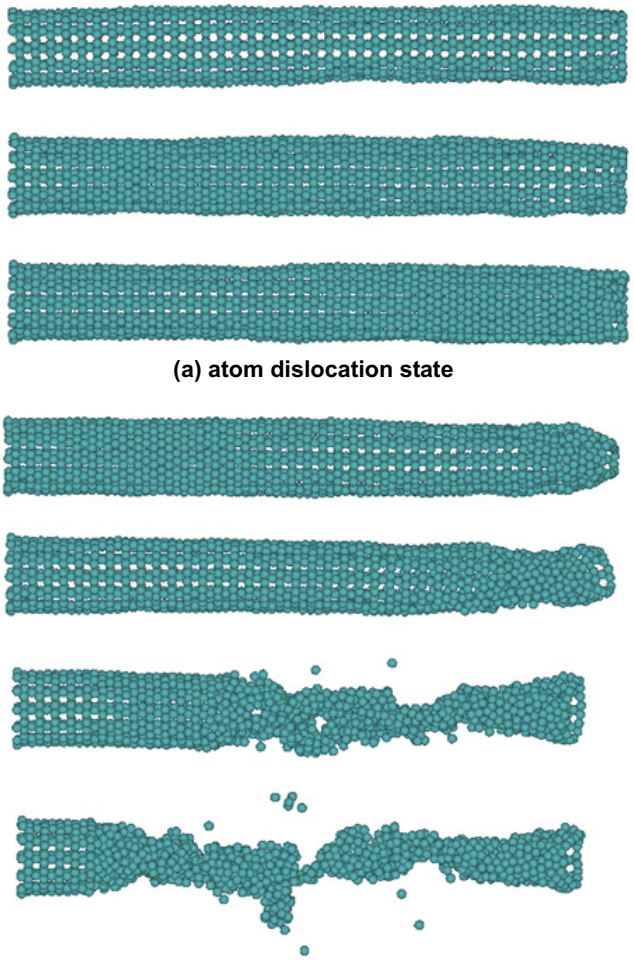

Figure 5. Structural evolution of SWCNT melting mechanism under thermal loading. Morphologies of structural growth sequences in single-wall carbon nanotubes corresponds to the thermal loading ~5.17 K Å^{-1}. (a) Denotes the initial state of the crack; one atom dislocated. The dislocation creates a pentagonal defect; (b) defect growth procedure.

(SWCNTs) under axial thermal loadings. The results of the present study enable the following conclusions to be drawn.

(1) It is shown that, given a thermal loading of sufficient intensity, the initial round cross section of the hot end of the nanotube transits to a flattened, rectangular configuration.

(2) The cross section oscillates between two fully perpendicular flattened states at a frequency which increases linearly with the intensity of the applied thermal load. This distinct periodic behavior can be used to realize tunable thermal pumping actuators.

(3) The diameter of the passing pore within the flattened SWCNT is smaller than that of the original cross section, but is independent of the intensity of the thermal load. The structural deformation of the SWCNT induced by the application of a thermal load can be exploited in active fluid transport devices for molecular selection.

(4) Deformation of the SWCNT under thermal treatment has two principal effects. In the initial regime, the dislocation atoms cause a pentagonal defect. Meanwhile, in the defect growth regime, the presence of an induced pentagonal defect in the tube acts as a driving force and are the leading defects promoting melting.

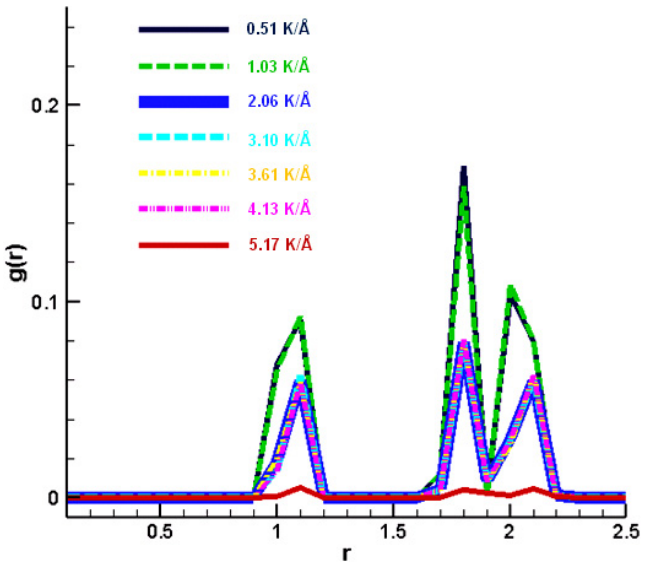

Figure 7. The radial distribution function at different thermal loadings in the melting process of SWCNTs.

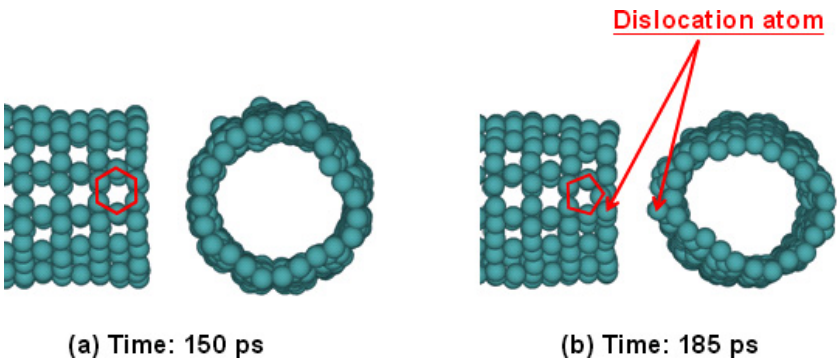

Figure 6. Pentagonal defect formation in SWCNTs. The nanotube cross section exhibits a atomic dislocation at the boundary and creates a pentagonal defect.

Acknowledgments

The authors gratefully acknowledge the financial support provided to this study by the Bureau of Energy, Taiwan, under contract no. 97-D0136.

References

[1] Dai H, Wong E W and Lieber C M 1996 *Science* **272** 523
[2] Ebbesen T W 1994 *Annu. Rev. Mater. Sci.* **24** 235
[3] Ebbesen T W, Lezec H J, Hiura H, Bennett J W, Ghaemi H F and Thio T 1996 *Nature* **382** 54
[4] Ajayan P M, Schadler L S, Giannaris C and Rubio A 2000 *Adv. Mater. (Weinheim, Ger.)* **12** 750
[5] Allaoui A, Bai S, Cheng H M and Bai J B 2002 *Compos. Sci. Technol.* **62** 1993
[6] Choi S U S, Zhang Z G, Yu W, Lockwood F E and Grulke E A 2001 *Appl. Phys. Lett.* **79** 2252
[7] Biercuk M J, Llaguno M C, Radosavljevic M, Hyun J K, Johonson A T and Fischer J E 2002 *Appl. Phys. Lett.* **80** 2767
[8] Dai L 2004 *Intelligent Macromolecules for Smart Device* (Berlin: Springer)
[9] Salvetat J P, Bonard J M, Thomson N H, Kulik A J, Forro L, Benoit W and Zuppiroli L 1999 *Appl. Phys.* A **69** 255
[10] Calvert P 1999 *Nature* **399** 210
[11] Chen R J, Zhang Y, Wang D and Dai H 2001 *J. Am. Chem. Soc.* **123** 3838
[12] Collins P G and Avouris P 2000 Nanotubes for electronics *Sci. Am.* **283** 38–45
[13] Chopra N G, Benedict L X, Crespi V H, Cohen M L, Louie S G and Zettl A 1995 *Nature* **377** 135–8
[14] Tu M F, Kowalewski T and Rouff R S 2001 *Phys. Rev. Lett.* **86** 87–90
[15] Zhang P H and Crespi V H 1999 *Phys. Rev. Lett.* **83** 1791–4
[16] Rotkin S V and Gogotsi Y 2002 *Mater. Res. Innov.* **5** 191–200
[17] Rappè A K, Casewit C J, Colwell K S, Goddard W A III and Skiff W M 1992 *J. Am. Chem. Soc.* **114** 10024–35
[18] Haile J M 1992 *Molecular Dynamic Simulation* (New York: Wiley)
[19] Müller-Plathe F 1997 *J. Chem. Phys.* **106** 6082–5
[20] Padgett C W and Brenner D W 2004 *Nano Lett.* **4** 1051–3
[21] López M J, Rubio A and Alonso J A 2003 arXiv:cond-mat/0303648v1
[22] Wu G and Li B 2007 arXiv:0707.4241v1
[23] Chen C H and Lee Y C 2007 *J. Micromech. Microeng.* **17** 1252–6
[24] Tuzun R E, Noid D W, Sumptr B G and Merkle R C 1997 *Nanotechnology* **8** 112
[25] Guo Y, Karasawa N and Goddard W A 1991 *Nature* **351** 464
[26] Richert R and Blumen A (ed) 1994 *Disorder Effects on Relaxational Processes: Glasses, Polymers, Proteins* (New York: Springer)
[27] Thrower P A 1969 *Chemistry and Physics of Carbon* vol 5 ed P L Walker Jr (New York: Dekker) p 262
[28] Stone A J and Wales D J 1986 *Chem. Phys. Lett.* **128** 501
[29] Allen M P and Tildesley D J 1987 *Computer Simulation of Liquid* (Oxford: Clarendon)